Impact of shear and extensional stiffness on equilibrium configurations of elastic Cosserat rods

Joachim Linn[1], **Fabio Schneider-Jung**[1], **Michael Roller**[1], **Tomas Hermansson**[2]

[1] Department Mathematics for the Digital Factory
Fraunhofer ITWM
Fraunhofer-Platz 1, 67661 Kaiserslautern, Germany
(joachim.linn, fabio.schneider-jung, michael.roller)@itwm.fraunhofer.de

[2] Department Geometry and Motion Planning
Fraunhofer–Chalmers Centre FCC
Chalmers Science Park, SE-412 88 Gothenburg, Sweden
tomas.hermansson@fcc.chalmers.se

ABSTRACT

Nonlinear rods are functionally important components in many flexible multibody systems. In this contribution, the influence of the effective stiffness parameters $[EA]$ and $[GA]$ of a Cosserat rod that affect the extension of the centerline as well as transverse shearing of cross sections is investigated in equilibrium configurations, also in comparison with the extensional strains of an extensible Kirchhoff rod. Besides rough order of magnitude estimates, quantitatively accurate bounds of the respective strains are derived theoretically and validated in numerical simulations.

Keywords: Cosserat rods, effective stiffness parameters, extensional and shear strains.

1 Introduction

Geometrically exact rod models [1] occur in three different variants w.r.t. the kinematical properties of their configuration variables (see Fig. 1): *(i)* inextensible Kirchhoff rods, *(ii)* extensible Kirchhoff rods, and *(iii)* Cosserat rods. We refer to [3] for technical details on the kinematics and differential geometry of geometrically exact rods.

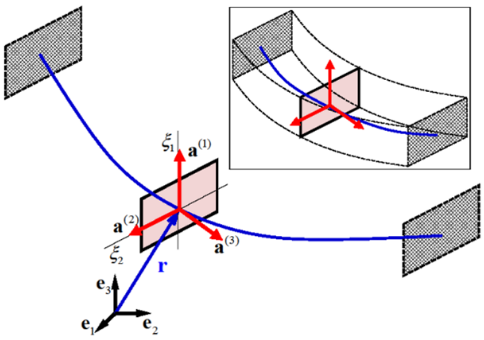

Figure 1. Centerline $\mathbf{r}(s)$ and moving frame $\mathsf{R}(s) = \mathbf{a}^{(k)}(s) \otimes \mathbf{e}_k$ of a Cosserat rod (see [3]).

We are interested in industrial applications where large spatial deformations of cables have to be simulated interactively [4]. Typical boundary conditions lead to deformed configurations showing a considerable amount of bending of the centerline, accompanied by a moderate amount of approximately uniform twisting of the cross sections along the configuration. In such cases, configurations computed by either of the three model variants turn out to be practically the same, as illustrated by Fig. 2:

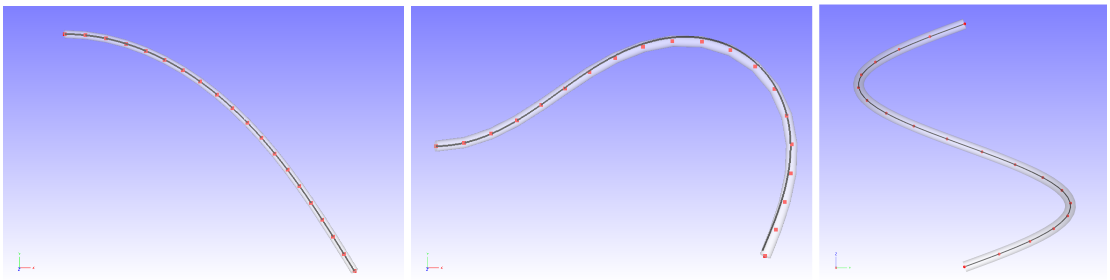

Figure 2. Analytical centerline curves of an inextensible Kirchhoff rod (solid lines) in plane bending (*left:* cantilever type, *middle:* both ends clamped) and helical (*right*) configurations. The red dots show the vertex positions computed with a discrete Cosserat rod model by minimization of the elastic energy (see [5] for details).

Bending and twisting are affected by the related effective stiffness parameters $[EI]$ and $[GJ]$, respectively. For composite cables, one needs to treat these stiffness parameters as independent quantities. Often the mass per length ρ_L of a cable is sufficiently low, such that the influence of gravity can be considered as weak, and the shape of deformed configurations in static equilibrium mainly depends on the ratio $[GJ]/[EI]$. Therefore it is important to measure these stiffness parameters properly [4, 6].

While for homogeneous elastic specimens the measurement of extensional stiffness $[EA]$ is an elementary experimental task, obtaining reproducible results from measurements of composite cables turns out to be far more difficult [6], and a measurement of the shear stiffness $[GA]$ is practically impossible. Therefore it is important to understand the influence of the effective stiffness parameters $[EA]$ and $[GA]$ on the rod configurations in equilibrium both qualitatively and quantitatively. Apart from the overall shape, estimates of the extensional strain $\varepsilon_t(s) := \|\mathbf{r}'(s)\| - 1$ and shear angle $\vartheta_s(s) := \arccos(\langle \mathbf{a}^{(3)}(s), \mathbf{t}(s)\rangle)$ are of interest, where $\mathbf{t}(s) := \mathbf{r}'(s)/\|\mathbf{r}'(s)\|$ is the unit tangent vector of the centerline.

In our contribution, we investigate the influence of the effective stiffness parameters $[EA]$ and $[GA]$ of a Cosserat rod model that govern extension (or compression) of the centerline as well as transverse shearing of the cross sections on its equilibrium configurations in such cases. Our results open up the possibility to *set* the stiffness parameters $[EA]$ and $[GA]$ to proper values by *modeling* rather than measurements.

2 Modelling details, methodical approach and theoretical a priori estimates

The sketch in Fig. 1 shows the centerline $\mathbf{r}(s)$ and moving frame $\mathsf{R}(s) = \mathbf{a}^{(k)}(s) \otimes \mathbf{e}_k$ of the configuration of a Cosserat rod. We refer to [3] for further technical details and mathematical notation.

The material tangent and curvature vectors $\mathbf{\Gamma}(s) := \mathsf{R}^T(s) \cdot \mathbf{r}'(s)$ and $\mathbf{K}(s) := \mathsf{R}^T(s) \cdot \boldsymbol{\kappa}(s)$ are strain measures that characterize the configuration geometry up to rigid body motions. They contain the components of the tangent vector $\mathbf{r}'(s)$ and the Darboux vector $\boldsymbol{\kappa}(s) = \frac{1}{2}\mathbf{a}^{(k)}(s) \times \mathbf{a}^{(k)\prime}(s)$ w.r.t. the local frame. The curve parameter $s \in [0, L]$ measures the arc length of the centerline in its reference configuration of length L, and derivatives w.r.t. s are denoted by a prime, e.g. $\mathbf{r}'(s) = \partial_s \mathbf{r}(s)$.

The moving frame $\mathsf{R}(s)$ is *adapted* to the centerline $\mathbf{r}(s)$ if $\Gamma^{(1,2)}(s) = \langle \mathbf{a}^{(1,2)}(s), \mathbf{r}'(s)\rangle \equiv 0$ for all $s \in [0, L]$, and $\Gamma^{(3)}(s) = \|\mathbf{r}'(s)\|$. For the Kirchhoff model variants *(i)* and *(ii)* one postulates that the moving frames $\mathsf{R}(s)$ remain adapted to the centerline also in deformed configurations, such that transverse shearing of the cross sections is inhibited. Variant *(i)* additionally postulates an inextensible centerline by requiring that $\|\mathbf{r}'(s)\| = 1$ holds for all deformed configurations. Differently, for variant *(iii)* neither adapted frames nor an inextensible centerline are assumed.

2.1 Scaling of the elastic energy terms and rough strain estimates

Assuming for simplicity zero gravity, equilibrium configurations of a straight inextensible Kirchhoff rod are local minima of its elastic bending and torsional energy, which in the case of transversally isotropic bending stiffness $[EI]$, torsional stiffness $[GJ]$ and cross sections with coinciding shear and area centers is given by $\mathscr{W}_{bt} = \frac{1}{2}\int_0^L ds\,[EI]\varkappa^2 + [GJ]\tau^2$, where $\varkappa(s)$ is the Frenet curvature of the inextensible centerline, and $\tau(s)$ is the twist of the adapted frame.

For extensible Kirchhoff rods, the total elastic energy consists of the sum $\mathscr{W}_{el} = \mathscr{W}_{bt} + \mathscr{W}_{ext}$ with the extensional energy $\mathscr{W}_{ext} = \frac{1}{2}\int_0^L ds\,[EA]\varepsilon_t^2$. For Cosserat rods, the latter is replaced by the more complex energy term $\mathscr{W}_{es} = \frac{1}{2}\int_0^L ds\,[EA]\Gamma_t^2 + [GA]\Gamma_s^2$ measuring the elastic energy stored in extension and transverse shearing, where the strains $\Gamma_s := \sqrt{\Gamma^{(1)2} + \Gamma^{(2)2}} = (1+\varepsilon_t)\sin(|\vartheta_s|) \approx |\vartheta_s|$ and $\Gamma_t := \Gamma^{(3)} - 1 = (1+\varepsilon_t)\cos(\vartheta_s) - 1 \approx \varepsilon_t$ depend on both deformation modes in a combined manner. The twist of a Cosserat rod is measured by the curvature component $K_t(s) \equiv K^{(3)}(s)$, and its total bending curvature by $K_b(s) := \sqrt{K^{(1)2} + K^{(2)2}} = \|\mathbf{a}^{(3)\prime}(s)\|$. These curvature quantities generalize the corresponding quantities $\tau(s)$ and $\varkappa(s) = \|\mathbf{t}'(s)\|$ of the Kirchhoff model, such that the elastic bending and torsional energy is given by $\mathscr{W}_{bt} = \frac{1}{2}\int_0^L ds\,[EI]K_b^2 + [GJ]K_t^2$.

Static equilibrium configurations of an elastic rod can be obtained as stable minima of its elastic energy (or more general: its potential energy including gravity, if the latter is present) subject to given boundary conditions. As a first step in our theoretical analysis of the impact of extensional and transverse shear stiffness on equilibrium configurations, we scale the various physical quantities that describe the model to characteristic values.

2.1.1 Characteristic scaling of the elastic energy terms

A rod of length L bent into a half circle has constant curvature $\varkappa = \pi/L$. This indicates that a curvature value of size $\varkappa_L := 1/L$ is rather moderate (for the half circle $\varkappa/\varkappa_L = \pi \approx 3$). On the other hand, for a circular cross section of radius r a local curvature of size $1/r$ or larger would geometrically imply self intersection. Even for a bit smaller curvature values in this range local strains become large, with substantial warping of the local cross sections, such that the rod model ceases to be a valid. Therefore $\varkappa \simeq 1/r$ corresponds to the range of extreme curvature values, while $\varkappa \simeq 1/L$ can be considered as the typical range of curvature values for moderate spatial deformations of slender rods. Below we outline how the introduction of L as the characteristic unit to measure length induces $\varkappa_L = 1/L$ as characteristic unit for curvature:

We introduce the dimensionless curve parameter $\bar{s} := s/L \in [0,1]$ for $s \in [0,L]$, the dimensionless centerline position vectors $\bar{\mathbf{r}}(\bar{s}) := \mathbf{r}(s)|_{s=L\bar{s}}/L$ and the respective frame directors $\bar{\mathbf{a}}^{(j)}(\bar{s}) := \mathbf{a}^{(j)}(s)|_{s=L\bar{s}}$, which are unit vectors and therefore already dimensionless quantities, all as functions of $\bar{s}$. First we note that $\mathbf{r}'(s) = \partial_s\mathbf{r}(s) = L(d\bar{s}/ds)\partial_{\bar{s}}\bar{\mathbf{r}}(\bar{s}) = \partial_{\bar{s}}\bar{\mathbf{r}}(\bar{s})$ holds, as $(d\bar{s}/ds) = 1/L$. As the tangent vectors of the two parametrisations $s \mapsto \mathbf{r}(s)$ and $\bar{s} \mapsto \bar{\mathbf{r}}(\bar{s})$ are identical at $s = L\bar{s}$, the same is also the case for the strain measures $\Gamma^{(j)}(s) = \langle \mathbf{r}'(s), \mathbf{a}^{(j)}(s)\rangle \equiv \langle \partial_{\bar{s}}\mathbf{r}(\bar{s}), \bar{\mathbf{a}}^{(j)}(\bar{s})\rangle =: \bar{\Gamma}^{(j)}(\bar{s})$ at $s = L\bar{s}$. Differently, the reparametrisation $s \mapsto \bar{s}$ affects the curvatures by rescaling them to the value $\varkappa_L = 1/L$, as the Darboux vector $\boldsymbol{\kappa}(s)$ and its scaled counterpart $\bar{\boldsymbol{\kappa}}(\bar{s}) = \frac{1}{2}\bar{\mathbf{a}}^{(k)}(\bar{s}) \times \partial_{\bar{s}}\bar{\mathbf{a}}^{(k)}(\bar{s})$ are related by the identity $\bar{\boldsymbol{\kappa}}(\bar{s}) = L\boldsymbol{\kappa}(s) = \boldsymbol{\kappa}(s)/\varkappa_L$ at $s = L\bar{s}$, and the scaled material curvature components are given by $\bar{K}^{(j)}(\bar{s}) = \langle \bar{\boldsymbol{\kappa}}(\bar{s}), \bar{\mathbf{a}}^{(j)}(\bar{s})\rangle = L\langle \boldsymbol{\kappa}(s), \mathbf{a}^{(j)}(s)\rangle = K^{(j)}(s)/\varkappa_L$. The scaled total bending curvature results as $\bar{K}_b(s) = K_b(s)/\varkappa_L$, and the scaled curvature quantities of the Kirchhoff model are obtained analogously as $\bar{\varkappa} = \varkappa/\varkappa_L$ and $\bar{\tau} = \tau/\varkappa_L$.

Using the scaled dimensionless quantities introduced above, the elastic energy terms likewise can be scaled to dimensionless form: $\bar{\mathscr{W}}_{bt} = \mathscr{W}_{bt}/W_{bt}^0$ and $\bar{\mathscr{W}}_{es} = \mathscr{W}_{es}/W_{es}^0$, with characteristic energy values $W_{bt}^0 := [EI]L\varkappa_L^2 = [EI]/L$ and $W_{es}^0 := [EA]L$, where we have assumed for simplicity that the effective stiffness parameters remain constant along the rod. The dimensionless energy terms are defined as $\bar{\mathscr{W}}_{bt} := \frac{1}{2}\int_0^1 d\bar{s}\,\bar{K}_b(\bar{s})^2 + \rho_{bt}\bar{K}_t(\bar{s})^2$ and $\bar{\mathscr{W}}_{es} := \frac{1}{2}\int_0^1 d\bar{s}\,\bar{\Gamma}_t(\bar{s})^2 + \rho_{es}\bar{\Gamma}_s(\bar{s})^2$, with the dimensionless ratios $\rho_{bt} := [GJ]/[EI]$ and $\rho_{es} := [GA]/[EA]$ of the effective stiffness parameters.

For the special case of a prismatic rod with circular cross section made of homogeneous, isotropic material the values of these ratios are $\rho_{bt} = 1/(1+\nu) = 2\rho_{es}$ with physical Poisson ratio values $0 \leq \nu \leq \frac{1}{2}$, which implies $\frac{2}{3} \leq \rho_{bt} \leq 1$ and $\frac{1}{3} \leq \rho_{es} \leq \frac{1}{2}$. For composite objects like cables, measured values of $[EI]$ and $[GJ]$ are found to be similar (i.e. $\rho_{bt} \approx 1$) in some cases, but one also finds cases where the structural properties of the cable components and their mechanical interaction lead to values $\rho_{bt} \simeq 10$, i.e. a substantially increased effective torsional stiffness compared to bending. Therefore in practise we need to consider a wider range of values of ρ_{bt} beyond $\rho_{bt} \approx 1$. As the shear stiffness $[GA]$ is practically not measurable, and measurements of the extensional stiffness $[EA]$ for composite cables are hampered by systematic difficulties caused by imperfect clamping, it is hard to make analogously reasonable statements about values of ρ_{es} observed in practise.

2.1.2 Rough estimates of the elastic energy terms and strains in equilibrium

If we consider spatial equilibrium states of an elastic rod like those shown in Fig. 2, the typical order of magnitude of the observed bending curvatures ranges from very small values in approximately straight sections up to largest values $K_b, \varkappa \simeq \varkappa_L$. The value of the twist of an elastic rod with isotropic bending stiffness in equilibrium is constant along the rod and depends on the boundary conditions: If none or only one of the ends of the rod is fully clamped, any equilibrium state of the rod is untwisted (see [2] Ch. II §19), otherwise typically values $K_t, \tau \simeq \varkappa_L$ occur.

Therefore we expect that roughly $\bar{\mathscr{W}}_{bt} \sim \mathscr{O}(1)$ holds in the cases of our interest. For boundary value problems leading to deformed configurations dominated by bending and torsion, one needs to find local minima of the scaled elastic energy $\bar{\mathscr{W}}_{el} = \mathscr{W}_{el}/W^0_{bt} = \bar{\mathscr{W}}_{bt} + \bar{\mathscr{W}}_{es}/\lambda_0^2$, where $\lambda_0^2 := [EI]/([EA]L^2) = W^0_{bt}/W^0_{es}$ is a small dimensionless parameter that can be estimated as $\lambda_0 \simeq \mathscr{O}(r_{IA}/L) \ll 1$ for the effective cross section radius $r_{IA} := 2\sqrt{I/A}$, as discussed below:

For slender prismatic elastic rods with a circular cross section of radius r made of homogeneous isotropic material $\lambda_0 = \frac{1}{2}r/L \ll 1$. More generally, one may extract the geometric dependencies of the effective stiffness values by defining effective elastic moduli $[E]_b := [EI]/I$ and $[E]_e := [EA]/A$ with ratio $\rho_E := [E]_b/[E]_e$, which takes the value $\rho_E = 1$ in the special homogeneous and isotropic case, and rewrite the definition of λ_0 in terms of these quantities as $\lambda_0^2 = \frac{1}{4}\rho_E(r_{IA}/L)^2$. As experiments show, composite cables react substantially stiffer in extension compared to bending, such that $\rho_E < 1$, and $\frac{1}{2}r_{IA}/L$ is an upper bound for λ_0.

On this basis, one may treat the energy minimization problem by Berdichevsky's method of variational asymptotic analysis [8, 9] to find approximate solutions for the Cosserat rod model, which to leading order coincide with those of the inextensible Kirchhoff model[1]. After the preparatory step to scale the elastic energy to its dimensionless form given by $\bar{\mathscr{W}}_{el} = \mathscr{W}_{el}/W^0_{bt} = \bar{\mathscr{W}}_{bt} + \bar{\mathscr{W}}_{es}/\lambda_0^2$ (see above), one would first search for rod configurations that minimize the leading term of order λ_0^{-2}, which results in $\bar{\mathscr{W}}_{es} \to 0$ by enforcing the Kirchhoff constraints (consistent with the boundary conditions), then subsequently minimize the term of order $\lambda_0^0 = 1$, i.e. the scaled energy $\bar{\mathscr{W}}_{bt}$, subject to the chosen boundary conditions, which yields the curvature $\varkappa(s)$ and twist $\tau(s)$ of the inextensible Kirchhoff solution. One recognizes by inspection (via counting powers of λ_0) that nonzero values of the extensional and shear strains can appear only in the next order of the asymptotic analysis, which besides $\varepsilon_t, \vartheta_s \sim \mathscr{O}(\lambda_0^2)$ also yields approximate curvature and twist values of the Cosserat model as those of the inextensible Kirchhoff model with additive corrections of order $\mathscr{O}(\lambda_0^2)$, i.e. $|K_b(s) - \varkappa(s)|/\varkappa_L, |K_t(s) - \tau(s)|/\varkappa_L = \mathscr{O}(\lambda_0^2)$. For the relative size of the elastic energy terms in equilibrium one finds the estimate $\mathscr{W}_{es} \simeq \lambda_0^2 \mathscr{W}_{bt}$.

Although a detailed exposition of the analytical computations sketched above is beyond the scope of this conference paper, we provide at least rough order of magnitude estimates $\varepsilon_t, \vartheta_s \sim \mathscr{O}(\lambda_0^2)$ for equilibrium values of both the extensional strains and shear angles by arguments brought for-

[1]We refer to [9] Vol. II, Part III, Ch. 15 for an application of this method to elastic beams, and Ex. 7 (p. 254-256) in section 5.11 of Vol. I, Part I, Ch. 5 for an elementary demonstration of the approach on the example of the bending energy terms of the linear Euler-Bernoulli and Timoshenko models.

ward by Audoly and Pomeau (see section 3.7 of [7]): Their *basic working hypothesis* is that for an elastic rod deformed by an external force F, *the order of magnitude of the bending moment M_b that balances the external force F is $M \simeq LF$*. Simple examples where this rough quantitative estimate holds are the moment acting at the clamped end of a cantilever beam, or a straight rod bent into the form of a helix of not too small radius and moderate pitch angle (see e.g. Fig. 2). The bending moment in a section of local curvature $\varkappa \simeq \varkappa_L = 1/L$ is $M_b \simeq [EI]/L$, which leads to the estimate $F \simeq [EI]/L^2$. In sections where the force locally acts approximately orthogonal to the cross sections, i.e. as a tension (or compressive) force $F_t = [EA]\varepsilon_t$, one obtains $\varepsilon_t \simeq [EI]/([EA]L^2) = \lambda_0^2$. If the force locally acts parallel to the cross sections as a shear force $F_s = [GA]\vartheta_s$, one obtains the analogous estimate $\vartheta_s \simeq \lambda_0^2$ with the assumption $[GA]/[EA] \simeq 1$. Evaluating the bending energy with curvatures $\varkappa \approx 1/L$ yields $\mathscr{W}_{bt} \approx \frac{1}{2}[EI]/L$. Inserting the estimates $\varepsilon_t, \vartheta_s \approx \lambda_0^2$ into the elastic energy term for extension and shearing (with $[GA] \approx [EA]$) results in $\mathscr{W}_{es} \approx \frac{1}{2}[EA]L\lambda_0^4 \approx \lambda_0^2\mathscr{W}_{bt}$. These rough estimates match the ones above resulting from variational asymptotic analysis.

2.2 Improved strain estimates obtained from the balance equations

In this section we further elaborate on the approach of Audoly and Pomeau [7]. We improve the rough estimates for extensional and shear strains of a Cosserat rod in equilibrium by considering the first integral $\mathbf{m} + \mathbf{r} \times \mathbf{f}$ of the equilibrium equations $\mathbf{f}' = \mathbf{0}$, $\mathbf{m}' + \mathbf{r}' \times \mathbf{f} = \mathbf{0}$, which hold for all rod model variants independent of kinematical constraints.

First we observe that for constant $\mathbf{f}$ the total moment $\mathbf{m}(s) + \mathbf{r}(s) \times \mathbf{f}$, which is likewise constant in equilibrium, provides the desired relation between the sectional moment $\mathbf{m}(s) = \mathbf{m}_b(s) + \mathbf{m}_t(s)$ and the "force times length" term $\mathbf{r}(s) \times \mathbf{f}$, which can be rewritten as $\mathbf{r}(s) \times \mathbf{f} = FL\bar{\mathbf{r}}(s) \times \hat{\mathbf{f}}$ with $\bar{\mathbf{r}}(s) := \mathbf{r}(s)/L$, $F = \|\mathbf{f}\|$ and $\hat{\mathbf{f}} := \mathbf{f}/F$. Note that even while $\mathbf{f}$ is constant along the rod, its orthogonal decomposition into the tension and shear force components $\mathbf{f}_t(s) = \langle \mathbf{a}^{(3)}(s), \mathbf{f}\rangle\, \mathbf{a}^{(3)}(s)$ and $\mathbf{f}_s(s) = \mathbf{a}^{(3)}(s) \times (\mathbf{f} \times \mathbf{a}^{(3)}(s)) = \mathbf{f} - \mathbf{f}_t(s)$ acting parallel and orthogonal to the cross section normal $\mathbf{a}^{(3)}(s)$ vary along the rod in its equilibrium configuration.

From $\mathbf{m}(s) + \mathbf{r}(s) \times \mathbf{f} = \mathit{const}$. we deduce that for any pair of positions $\mathbf{r}(s_{1,2})$ on the centerline of an equilibrium configuration the identity

$$\mathbf{m}(s_2) - \mathbf{m}(s_1) \;=\; \mathbf{f} \times (\mathbf{r}(s_2) - \mathbf{r}(s_1)) \tag{1}$$

holds for arbitrary $s_{1,2} \in [0, L]$. This will be the starting point of our derivation of improved quantitative estimates for the extensional and shear strains in equilibrium.

We pick a position $\mathbf{r}_0 := \mathbf{r}(s_0)$ on the centerline at some fixed $s_0 \in [0, L]$ (to be determined later) where the moment takes the value $\mathbf{m}_0 := \mathbf{m}(s_0)$. From the identity (1) we can deduce the equalities

$$\|\mathbf{m}(s) - \mathbf{m}_0\| \;=\; \|\mathbf{f} \times (\mathbf{r}(s) - \mathbf{r}_0)\| \;=\; F\,\|\hat{\mathbf{f}} \times \Delta\mathbf{r}(s)\|\,, \tag{2}$$

with direction $\hat{\mathbf{f}}$ and modulus F of the constant force $\mathbf{f}$ already introduced above, and the secant vector $\Delta\mathbf{r}(s) := \mathbf{r}(s) - \mathbf{r}_0$ between positions on the centerline.

For the inextensible Kirchhoff model the components $F_j(s) := \langle \mathbf{f}, \mathbf{a}^{(j)}(s)\rangle$ of the constant sectional force $\mathbf{f}$ w.r.t. the local frame act as Lagrange multipliers paired with the algebraic constraints $\Gamma^{(1,2)} = 0$ and $\Gamma_t = 0$ enforcing vanishing extensional and shear strains. For the extensible Kirchhoff model the tension force component is $\mathbf{f}_t(s) = [EA]\varepsilon_t(s)\mathbf{t}(s)$, such that the constant modulus of the sectional force is given by $F = \sqrt{([EA]\varepsilon_t(s))^2 + f_s(s)^2}$, with the modulus $f_s(s) = \|\mathbf{f}_s(s)\|$ of the shear force obtained from the vector Lagrange multiplier $\mathbf{f}_s(s) = F_\alpha(s)\mathbf{a}^{(\alpha)}(s)$ related to the constraints $\Gamma^{(1,2)}(s) = 0$. For the Cosserat model the shear force is obtained from the constitutive relation $\mathbf{f}_s(s) = [GA]\Gamma^{(\alpha)}(s)\mathbf{a}^{(\alpha)}(s)$ with modulus $f_s(s) = [GA]\Gamma_s(s)$, and $F = \sqrt{([EA]\Gamma_t(s))^2 + ([GA]\Gamma_s(s))^2} = [EA]\bar{F}$ with $\bar{F} := \sqrt{\Gamma_t(s)^2 + \rho_{es}^2\Gamma_s(s)^2} = F/[EA]$.

We may likewise scale the sectional moment $\mathbf{m}(s)$ by a characteristic moment quantity. The obvious candidate for the latter is $[EI]\varkappa_L = [EI]/L$, which yields $\bar{\mathbf{m}}(s) := \mathbf{m}(s)/([EI]\varkappa_L)$ as dimensionless moment vector. For the constitutive relation $\mathbf{m}(s) = [EI]\varkappa(s)\mathbf{b}(s) + [GJ]\tau(s)\mathbf{t}(s)$ of an inextensible Kirchhoff rod with straight untwisted reference configuration this scaling yields $\bar{\mathbf{m}}(s) = \bar{\varkappa}(s)\mathbf{b}(s) + \rho_{bt}\,\bar{\tau}(s)\mathbf{t}(s)$. This illustrates the effect of normalizing the moment to $[EI]/L$.

As F is constant in equilibrium, the ratio of the terms $\|\mathbf{m}(s) - \mathbf{m}_0\|$ and $\|\hat{\mathbf{f}} \times \Delta\mathbf{r}(s)\|$ appearing on both sides of (2) is likewise constant along the rod. For all $s \in [0, L]$ where $\|\hat{\mathbf{f}} \times \Delta\mathbf{r}(s)\| \neq 0$ we can rewrite the identity above in the form

$$\sqrt{f_t(s)^2 + f_s(s)^2} \;=\; F \;=\; \frac{\|\mathbf{m}(s) - \mathbf{m}_0\|}{\|\hat{\mathbf{f}} \times \Delta\mathbf{r}(s)\|} \;=:\; \Lambda_{[\mathbf{m},\mathbf{f},\mathbf{r}]}(s) \;=\; const. \tag{3}$$

with $f_t(s) = [EA]\,\varepsilon_t(s)$ or ε_t replaced by $\Gamma_t(s)$ and $f_s(s) = [GA]\,\Gamma_s(s)$ for the extensible Kirchhoff and Cosserat model variants respectively. The cases when $\|\hat{\mathbf{f}} \times \Delta\mathbf{r}(s)\| \to 0$, i.e. if the secant vector $\mathbf{r}(s) - \mathbf{r}_0$ becomes (anti)parallel to the force $\mathbf{f}$, or for $\mathbf{r}(s) \to \mathbf{r}_0$, are removable singularities, as then $\|\mathbf{m}(s) - \mathbf{m}_0\| \to 0$ as well, such that the value of the quotient $\Lambda_{[\mathbf{m},\mathbf{f},\mathbf{r}]}$ equals F.

The l.h.s. of the identity (3) can now be utilized to obtain a sharp inequality estimate of the modulus of either the extensional strain or the shear strain by setting either $f_t(s) \equiv 0$ or $f_s(s) \equiv 0$. This either leads to $F \geq [EA]\,|\varepsilon_t(s)|$ resp. $F \geq [EA]\,|\Gamma_t(s)|$ or $F \geq [GA]\,\Gamma_s(s)$. Equality holds whenever the extensional or the shear force component vanish locally. In terms of scaled dimensionless quantities (3) can be rewritten equivalently as

$$|\Gamma_t(s)|\,,\; \rho_{es}\Gamma_s(s) \;\leq\; \sqrt{\Gamma_t(s)^2 + \rho_{es}^2\Gamma_s(s)^2} \;=\; \bar{F} \;=\; \lambda_0^2\,\frac{\|\bar{\mathbf{m}}(s) - \bar{\mathbf{m}}_0\|}{\|\hat{\mathbf{f}} \times \Delta\bar{\mathbf{r}}(s)\|} \;=\; \lambda_0^2\,\bar{\Lambda}_{[\mathbf{m},\mathbf{f},\mathbf{r}]}\;, \tag{4}$$

where $\Delta\bar{\mathbf{r}}(s) := (\mathbf{r}(s) - \mathbf{r}_0)/L$ is the normalized secant vector, and $\bar{\Lambda}_{[\mathbf{m},\mathbf{f},\mathbf{r}]}(s) := [EI]/L^2\,\Lambda_{[\mathbf{m},\mathbf{f},\mathbf{r}]}(s)$. Note that on the r.h.s. of (4) the small parameter $\lambda_0^2 = [EI]/([EA]L^2) \simeq (r/L)^2$ appears. This confirms the (rough) estimates suggested in the previous subsection, provided that $\bar{\Lambda}_{[\mathbf{m},\mathbf{f},\mathbf{r}]} \simeq \mathcal{O}(1)$.

For an extensible Kirchhoff rod we obtain $|\varepsilon_t(s)| \leq \lambda_0^2\bar{\Lambda}_{[\mathbf{m},\mathbf{f},\mathbf{r}]}$ as an estimate of the extensional strain in equilibrium. The corresponding estimate for $|\vartheta_s| \approx \Gamma_s = (1 + \varepsilon_t)\sin(|\vartheta_s|)$ results analogously, with an additional factor $1/\rho_{es} = [EA]/[GA]$ on the r.h.s..

The actual numerical value of the constant term $\bar{\Lambda}_{[\mathbf{m},\mathbf{f},\mathbf{r}]}$ depends on a particular equilibrium solution of the concrete boundary value problem considered. Moreover, the terms $\|\bar{\mathbf{m}}(s) - \bar{\mathbf{m}}_0\|$ and $\|\hat{\mathbf{f}} \times \Delta\bar{\mathbf{r}}(s)\|$ in the numerator and denominator of the definition of $\bar{\Lambda}_{[\mathbf{m},\mathbf{f},\mathbf{r}]}$ on the r.h.s. of (4) are of qualitatively rather different nature: While the former depends on the evolution of the state of bending and twisting curvature along the rod, or more precisely the change of these curvatures, the latter depends on the shape of the centerline curve $\mathbf{r}(s)$ in terms of its secant vectors $\Delta\mathbf{r}(s)$ relative to the constant *direction* $\hat{\mathbf{f}}$ of the sectional force (but *not* on its magnitude $F = \|\mathbf{f}\|$).

This makes it feasible to derive a generic estimate of the former quantity, while a reasonable estimate for the latter is (in practise) not readily available. Starting e.g. from the scaled constitutive relation $\bar{\mathbf{m}}(s) = \bar{\varkappa}(s)\mathbf{b}(s) + \rho_{bt}\,\bar{\tau}(s)\mathbf{t}(s) = \bar{\mathbf{m}}_b(s) + \bar{\mathbf{m}}_t(s)$ for a Kirchhoff rod given above, one finds the "worst case" estimate $\|\bar{\mathbf{m}}(s) - \bar{\mathbf{m}}_0\|/2 \leq \bar{\varkappa}_{max} + \rho_{bt}\,\bar{\tau}_0$, where $\bar{\varkappa}_{max}$ is the maximum bending curvature of the equilibrium solution, and $\bar{\tau}_0$ its constant twist, both in units of $\varkappa_L$. It is well known that for nonlinear rod models there often exist multiple equilibrium solutions of different spatial shape for the same (or similar) sectional forces and moments. This prevents us to make a comparably "educated guess" for the quantity $\|\hat{\mathbf{f}} \times \Delta\bar{\mathbf{r}}(s)\|$ that proves to be generally valid.

Altogether, these considerations indicate that it is neither straightforward nor feasible to derive a generally valid estimate of the term $\bar{\Lambda}_{[\mathbf{m},\mathbf{f},\mathbf{r}]}$ valid for a wider class of boundary value problems of practical interest. However, values of $\bar{\Lambda}_{[\mathbf{m},\mathbf{f},\mathbf{r}]}$ can be obtained from numerical solutions. This will be investigated further in the examples presented in the following section.

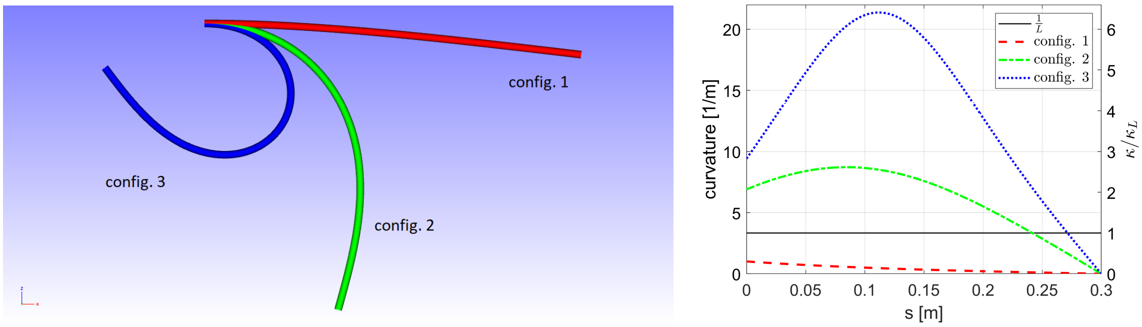

Figure 3. *Left*: Three different example configurations, all with plane bending. *Right*: Curvature along the rod with two different y-axes (in [1/m] and dimensionless in units of $\varkappa_L$). Numerical solutions are computed by minimization of the elastic energy subject to the prescribed boundary conditions(see [5] for details).

3 Some illustrative numerical examples

The estimates derived in the previous subsection are in general applicable to a wide class of spatial equilibrium configurations of a nonlinear rod for boundary conditions that do not enforce stretching as the main deformation mode or induce sharp local bending with extreme curvature values. The main impact of large spatial deformations of a rod (i.e. large displacements of centerline positions and large rotations of the cross section orientations) on stretching and shearing can be studied already in situations of plane bending with zero torsion, as the latter influences the extensional and shear strains merely in a quantitative manner, but does not induce any qualitatively new effects.

To illustrate the validity of both the rough and the improved estimate of the extensional strain, we first investigate three different configurations (see Fig. 3) of an extensible Kirchhoff rod with parameters given in Table 1.

L	r	$[EI]$	$[EA]$	$[GJ]$
300mm	3mm	0.02Nm^2	10000N	0.05Nm^2

Table 1. Parameters for numerical examples with the extensible Kirchhoff rod, corresponding to a numerical value of $\lambda_0^2 = \frac{2}{9} \cdot 10^{-4}$ (or $\lambda_0 \approx 0.47 \cdot 10^{-2} < r/L = 10^{-2}$).

The effective stiffness parameters $[EI]$, $[GJ]$ and $[EA]$ were independently set to typical stiffness values for electrical cables. Moreover, to meet the assumption in the theoretical investigations, gravity was neglected.

Each configuration represents a case of plane bending (in the x-y-plane), where one end of the rod ($s = 0$mm) is fully clamped while the other end ($s = L$) is kept moment-free. Consequently, also the curvature vanishes at $s = L$. From Fig. 3 one can observe, that for the first configuration the curvature is strictly smaller than $\varkappa_L = 1/L$, while maximum curvature is considerably larger for the second and third configuration.

In Fig. 4, the simulated extensional strains of all configurations are plotted, together with the rough estimate λ_0^2 (equal for all configurations), which approximately sets the order of magnitude for the strains, and the improved estimate $\lambda_0^2 \bar{\Lambda}_{[\mathbf{m},\mathbf{f},\mathbf{r}]}$. Obviously, $\bar{\Lambda}_{[\mathbf{m},\mathbf{f},\mathbf{r}]}$ increases with increasingly stronger curved configurations and always leads to a value for $\lambda_0^2 \bar{\Lambda}_{[\mathbf{m},\mathbf{f},\mathbf{r}]}$ which fits well to the maximum occurring extensional strain.

Note that already for the weakly curved configuration No. 1 (with all curvature values below $\varkappa_L$), the maximum extensional strain is significantly larger than its roughly estimated value λ_0^2, as even

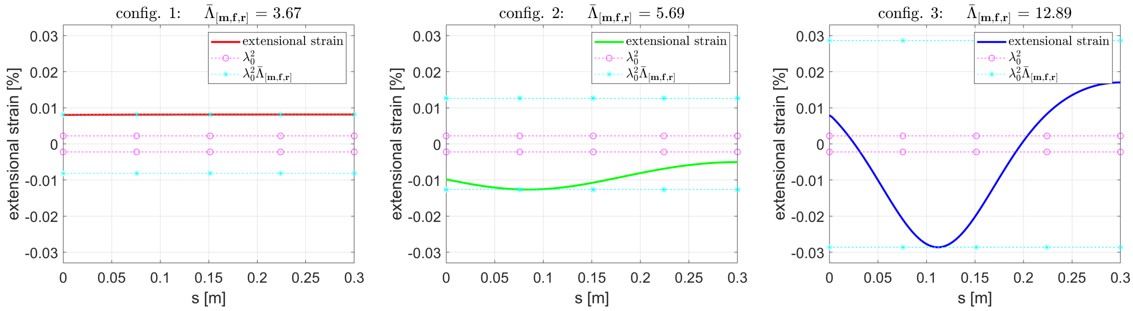

Figure 4. Simulated extensional strain (*left*: config. 1, *middle*: config. 2, *right*: config. 3), together with rough estimate λ_0^2 and improved estimate $\lambda_0^2\bar{\Lambda}_{[\mathbf{m,f,r}]}$.

in that case the factor $\bar{\Lambda}_{[\mathbf{m,f,r}]}$ is not close to 1 as expected, but takes a numerical value of 3.67. In configuration No. 3, the most strongly curved configuration shown in Fig. 3, the maximum value of the bending curvature approximately corresponds to a a curvature radius of 8 cross section diameters (more precisely: $\varkappa_{max} = 21.73\,m^{-1} \;\Rightarrow\; 1/(2r\,\varkappa_{max}) = 7.8$). Curvatures in this range are typical in automotive applications, where design guidelines for cable layouts require that curvature radii should not be smaller than a few cross section diameters. Therefore configuration No. 3 can still be considered as moderately strong curved from the application point of view. Extensional strains are still tiny in this case, however a correction factor of $\bar{\Lambda}_{[\mathbf{m,f,r}]} \approx 13$ yields an improved strain estimate with bounds that are an order of magnitude larger than those of the rough one.

Next, to also analyze the estimates for shear strain, we use a discrete Cosserat rod model and set $[GA] = [EA]$ for the additional effective shear stiffness (leading to $\rho_{es} = 1$).

The rod configurations and corresponding curvatures and extensional strains are practically indistinguishable from those shown in Fig. 3 and Fig. 4. Of course, the numerical values are not identical in detail, as two different discrete rod models are used, and the simulation method consists of an iterative optimization procedure applied to energy minimization, such that it is difficult to assign solution differences to differences in the model in the presence of differences due to numerical approximations. Therefore we don not show the respective plots of these results, and also do not attempt to analyze differences in the simulation results of the aforementioned quantities.

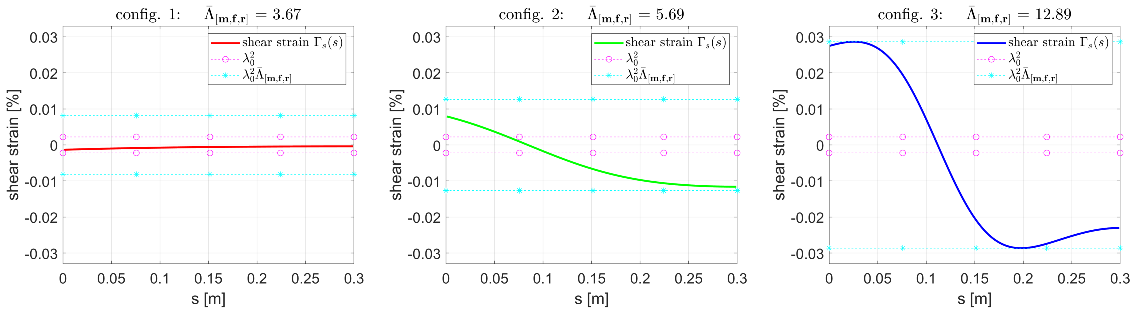

Figure 5. Simulated shear strain (*left*: config. 1, *middle*: config. 2, *right*: config. 3), together with rough estimate λ_0^2 and improved estimate $\lambda_0^2\bar{\Lambda}_{[\mathbf{m,f,r}]}$.

The transverse shear strains obtained from the discrete Cosserat rod model are plotted in Fig. 5. Note that the plotted quantity is not Γ_s, but the non-vanishing shear strain component $\Gamma^{(1)}(s)$, which is a signed quantity. (The other component $\Gamma^{(2)}(s)$ vanishes identically for plane bending.)

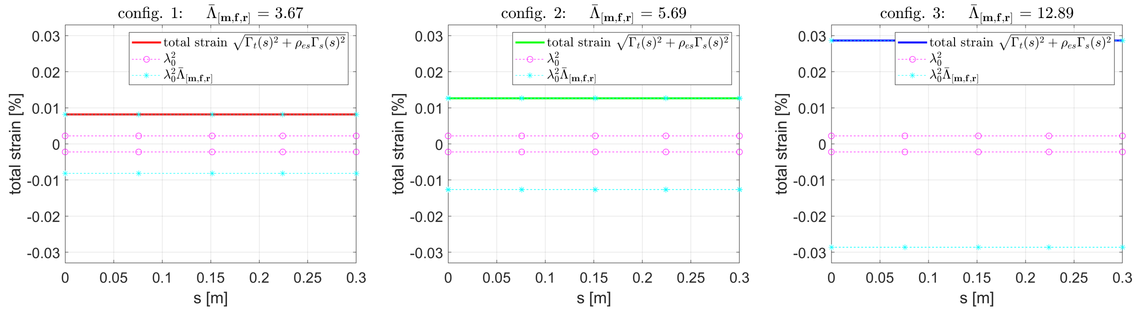

Figure 6. Simulated total extensional & shear strain values (*left*: config. 1, *middle*: config. 2, *right*: config. 3), together with rough estimate λ_0^2 and improved estimate $\lambda_0^2\bar{\Lambda}_{[\mathbf{m},\mathbf{f},\mathbf{r}]}$.

According to (4) the shear strains should be bounded by the same limits as the extensional strains. For the stronger curved configurations No. 2 and 3 the numerical values exceed the narrow bounds $\pm\lambda_0^2$ of the rough estimate but stay within the wider bounds $\pm\lambda_0^2\bar{\Lambda}_{[\mathbf{m},\mathbf{f},\mathbf{r}]}$. For the weakly curved configuration No. 1 one observes that the shear strains stay within the narrow bounds $\pm\lambda_0^2$.

For completeness we also show in Fig. 6 the simulated values of the total extensional & shear strain $\bar{F} = \sqrt{\Gamma_t(s)^2 + \rho_{es}^2\Gamma_s(s)^2}$, which exactly matches the theoretically predicted value $\bar{F} = \lambda_0^2\,\bar{\Lambda}_{[\mathbf{m},\mathbf{f},\mathbf{r}]}$ given in (4) for an equilibrium configuration of a Cosserat rod, and indirectly also shows that both $\mathbf{f}(s)$ and $\mathbf{m}(s) + \mathbf{r}(s) \times \mathbf{f}(s)$ are indeed constant quantities in equilibrium.

Altogether the examples of plane bending indicate that although the order of magnitude of the extensional and shear strains is roughly given by the small parameter $\lambda_0^2 \simeq (r/L)^2$, the improved bounds $\pm\lambda_0^2\bar{\Lambda}_{[\mathbf{m},\mathbf{f},\mathbf{r}]}$ according to (4) yield quantitative information that is consistently more accurate than the one obtained from the rough order of magnitude estimates.

4 Conclusions

In this contribution we systematically investigated the influence of the effective stiffness parameters $[EA]$ and $[GA]$ of a Cosserat rod as well as an extensible Kirchhoff rod on the size of the extensional and shear strains in equilibrium configurations showing moderate bending of the centerline and twisting of the cross sections.

After choosing the rod length L as characteristic unit of length, which induces $\varkappa_L = 1/L$ as characteristic unit of curvature, we identified $\lambda_0^2 = [EI]/([EA]L^2)$, which equals $\frac{1}{4}\frac{r^2}{L^2}$ in the well known special case of a homogeneous elastic rod with circular cross section of radius r, as the small parameter that roughly determines the order of magnitude of both extensional and shear strains in equilibrium. Taking the static equilibrium equations for the sectional force and moment vectors $\mathbf{f}(s)$ and $\mathbf{m}(s)$ of the rod as a starting point, and assuming that no external forces and moments act on the rod, we were able to derive quantitatively sharp estimates for the extensional and shear strains, with improved bounds $\pm\lambda_0^2\bar{\Lambda}_{[\mathbf{m},\mathbf{f},\mathbf{r}]}$ given by the constant, yet configuration dependent dimensionless parameter $\bar{\Lambda}_{[\mathbf{m},\mathbf{f},\mathbf{r}]}$, for which we observed numerical values in the range $\bar{\Lambda}_{[\mathbf{m},\mathbf{f},\mathbf{r}]} \approx 5\ldots15$ even for weakly to moderately strong curved configurations in plane bending.

Our investigations can (and should) be extended w.r.t. various aspects:

At first, we expect that for spatial deformations the values of the parameter $\bar{\Lambda}_{[\mathbf{m},\mathbf{f},\mathbf{r}]}$ are similar to those observed in plane bending with the same range of centerline curvatures, and that a small to moderate amount of nonzero twist only adds a likewise small to moderate quantitative correction to this. This needs to be verified in corresponding numerical experiments.

Next one should include gravity into the investigation. In this case $\mathbf{f}(s)$ varies linearly along the rod, such that $\bar{\Lambda}_{[\mathbf{m},\mathbf{f},\mathbf{r}]}(s)$ also is no longer a constant parameter. Nevertheless, we expect that the bounds $\pm\lambda_0^2\bar{\Lambda}_{[\mathbf{m},\mathbf{f},\mathbf{r}]}(s)$ are still quantitatively correct for cases where gravity is not a dominant effect for the overall deformation of the rod.

Moreover, we think it should be possible to estimate the dependence of $\bar{\Lambda}_{[\mathbf{m},\mathbf{f},\mathbf{r}]}$ on the particular equilibrium configuration in terms of characteristic solution properties, e.g. the maximum bending curvature. This could be utilized to derive "worst case" estimates of the extensional and shear strains for a wider class of configurations that are less sharp than $\pm\lambda_0^2\bar{\Lambda}_{[\mathbf{m},\mathbf{f},\mathbf{r}]}$, but more accurate than the rough order of magnitude estimate $\pm\lambda_0^2$.

Finally, we want to address the issue that for cables the effective stiffness parameter $[EA]$ is hard to measure due to systematic limitations of the experimental setup, and $[GA]$ is not measurable in practise at all. Our results point out that it might make sense to *set* these parameters rather than measuring them, to "favorable" values that still lead to acceptably small extensional and shear strains, in the sense that the geometry of the deformed rod configuration remains correct, and the sectional forces and moments are still close to the ones obtained from an inextensible Kirchhoff rod model.

REFERENCES

[1] Antman, S.S.: *Nonlinear Problems of Elasticity*. Springer (2005).

[2] Landau, L.D., Lifshitz, E.M.: *Course of Theoretical Physics Vol. 7: Theory of Elasticity (3rd edition)*. Butterworth-Heinemann (1986).

[3] J. Linn: Discrete Cosserat Rod Kinematics Constructed on the Basis of the Difference Geometry of Framed Curves — Part I: Discrete Cosserat Curves on a Staggered Grid. *Journal of Elasticity*, Vol. **139**, pp. 177–236 (2020).

[4] J. Linn, F. Schneider, K. Dreßler, O. Hermanns: Virtual Product Development and Digital Validation in Automotive Industry. In Bock, H.G., Küfer, KH., Maass, P., Milde, A., Schulz, V. (eds): *German Success Stories in Industrial Mathematics*. Mathematics in Industry, vol. **35**, pp. 45-54, Springer (2021)

[5] J. Linn, T. Hermansson, F. Andersson, F. Schneider: Kinetic aspects of discrete Cosserat rods based on the difference geometry of framed curves. In M. Valasek et al. (Eds.): Proceedings of the *ECCOMAS Thematic Conference on Multibody Dynamics 2017*, pp. 163–176, 2017.

[6] Dörlich, V., Linn, J., Diebels, S.: Flexible beam-like structures—experimental investigation and modeling of cables. In: Altenbach, H., et al. (eds.): *Advances in Mechanics of Materials and Structural Analysis. Advanced Structured Materials*, vol. **80**, pp. 27–46, Springer (2018).

[7] Audoly, B., Pomeau, Y.: *Elasticity and Geometry — From hair curls to the non-linear response of shells*. Oxford UP (2010).

[8] Berdichevsky, V.L.: On the energy of an elastic rod. *J. Appl. Math. Mech. (PMM)* **45**(4), pp. 518–529 (1981).

[9] Berdichevsky, V.L.: *Variational Principles of Continuum Mechanics, Vol. I: Fundamentals, Vol. II: Applications*. Springer (2009).